TECHNICAL AND ENVIRONMENTAL EVALUATION OF USING RICE HUSKS AND SOLAR ENERGY ON THE ACTIVATION OF ABSORPTION CHILLERS IN THE CARIBBEAN REGION. CASE STUDY: BARRANQUILLA

/

EVALUACIÓN TÉCNICA Y AMBIENTAL DEL USO DE CÁSCARA DE ARROZ Y ENERGÍA SOLAR EN LA ACTIVACIÓN DE REFRIGERADORES DE ABSORCIÓN EN LA REGIÓN CARIBE. CASO DE ESTUDIO: BARRANQUILLA

Andrés Rodríguez Toscano*[1)], Rafael Ramirez[2)], José M. Sánchez[2)]
[1)]Universidad de la Costa, Energy Department, Cl. 58 #55-66, 080002 Barranquilla, Colombia/ Colombia;
[2)]Universidad del Atlántico, Efficient Energy Management Research Group-Kai, Carrera 30 Número 8-49, 081007 Puerto Colombia/ Colombia.
Tel: +573004162429; E-mail: arodrigu83@cuc.edu.co
DOI: https://doi.org/10.35633/inmateh-70-06

Keywords: *Absorption refrigeration system, solar energy, biogas, biomass, solar cooling, rice husk.*

ABSTRACT

This research presents a thermodynamic analysis of a Thermal LTC-10 single-effect absorption series cooling system using the water/LiBr pair. Four operating scenarios were modeled on an hourly basis (24h) with EES software using mass and energy balances and the environmental conditions of the city of Barranquilla, Colombia. The analysis of the results shows that the system powered only by solar energy obtains the highest COP between 8:00 and 16:00 hours and the lowest greenhouse gas (GHG) emissions, while the system powered by rice husk biogas presents stable operation throughout the day and higher SO_2eq emissions.

RESUMEN

En esta investigación se presenta un análisis termodinámico de un sistema de refrigeración en serie por absorción de simple efecto Thermal LTC-10 utilizando el par agua/LiBr. Cuatro escenarios de operación fueron modelados en una base horaria (24h) con el software EES utilizando balances de masa y energía y las condiciones ambientales de la ciudad de Barranquilla, Colombia. El análisis de los resultados demuestra que el sistema alimentado únicamente por energía solar obtiene el mayor COP entre las 8:00 y las 16:00 horas y las menores emisiones de gases de efecto invernadero (GEI), mientras que el sistema alimentado con biogás de cáscara de arroz presenta un funcionamiento estable durante todo el día y mayores emisiones de SO_2eq.

INTRODUCTION

Despite the efforts to reduce the energy consumption and greenhouse gas emissions, these continue to increase (*IEA, 2019; Li et al., 2022; Saint Kadir et al., 2020*). Therefore, it is very interesting for researchers to analyze the possibility of replacing traditional sources with renewable energy sources (*Ghafoor & Munir, 2015; IEA, 2019; A. R. Toscano et al., 2020*). HVAC systems account for about 40% of the electrical energy consumed in buildings globally (*Aune et al., 2016; Pérez-Lombard et al., 2008; Rodríguez-Toscano et al., 2022a)*. Therefore, these systems are often energy-intensive, especially in the operation of the compressor, which coupled with leaks, lack of maintenance and cleaning can lead to a significant increase in energy consumption (*Adel et al., 2016; Juaidi et al., 2016; Rodríguez-Toscano et al., 2022a*).

In the specialized literature, the solar energy equipment to activate cooling systems has been reported (*Allouhi et al., 2015; Asadi et al., 2018*). Other studies have used these technologies with absorption refrigeration systems to reduce the use of electricity and take advantage of residual thermal energy in the industrial sector (*Asadi et al., 2018; Bellos & Tzivanidis, 2017; United States Department of Energy, 2016*). Further research has demonstrated the feasibility of solar-powered absorption cooling systems in shopping malls by means of different working fluids to improve the heat transfer and COP with computational sources, experiments, and tests in commercial facilities (*Alhamid et al., 2020; Amaris, 2013; Rodríguez-Toscano et al., 2022a; Zapata et al., 2021*). However, there is scarce information available on absorption refrigeration systems installed on the market that involves biomass as another energy source for their activation, along with the use of solar energy (*Ayou et al., 2013; Ghafoor & Munir, 2015; A. D. R. Toscano et al., 2021*).

Colombia has an energy potential from solar and biomass sources *(Sagastume Gutiérrez et al., 2020; UPME, 2015*). In this country, the energy produced with biomass for self-generation and cogeneration purposes is higher than solar and wind energy (*Federación Nacional de Biocombustibles de Colombia, 2018*).

Rice is the third most-produced human-consumable agricultural product in Colombia, with more than 2,463,689 tons/year (*UPME, 2016a*). From this, residual biomass called rice husk is obtained, which has an energy potential of approximately 7,136.53 TJ/year (*UPME, 2016a*). On the other hand, the Colombian Caribbean coast has a high solar energy potential with average solar irradiation of approximately 5 kW-h/m^2, with high relative humidity and average ambient temperatures of up to 35ºC (*Castro, 2010; EPM, 2020; Rodríguez-Toscano et al., 2022b; UPME, 2015; Weather Underground, 2020*). This involves using cooling systems for air conditioning and industrial sector needs. Nevertheless, the potential of this biomass has not been studied in conjunction with solar energy in absorption cooling systems, which generates uncertainty about the use of this energy source in terms of operation, air pollution, and system performance in companies or industries that have these agricultural residues and are located on the Colombian Caribbean coast.

MATERIALS AND METHODS

This section describes the environmental characteristics of the city of Barranquilla, the thermodynamic model, and the economic model of the absorption cooling system using biomass (rice husk) and the solar energy as activation source considering water/LiBr as the working pair in the simulation of the absorption refrigeration system.

ENVIRONMENTAL VARIABLES IN BARRANQUILLA

The city of Barranquilla is characterized by maintaining a high solar potential on the Colombian Caribbean coast. Its ambient temperature is between 24ºC and 35ºC (*Castro, 2010; EPM, 2020; Rodríguez-Toscano et al., 2022b; Weather Underground, 2020*). Figure 1 shows the behavior of the average solar irradiance for a day (24 h) in the months of February and October. Where it is noticeable that February is the month of highest solar irradiance and October the month of lowest solar irradiance. Also, the irradiation peaks occur between 9:00 and 15:00 hours. In this sense, the requirements for activating the solar absorption regeneration system during peak hours will be considered from the month with the lowest solar irradiation.

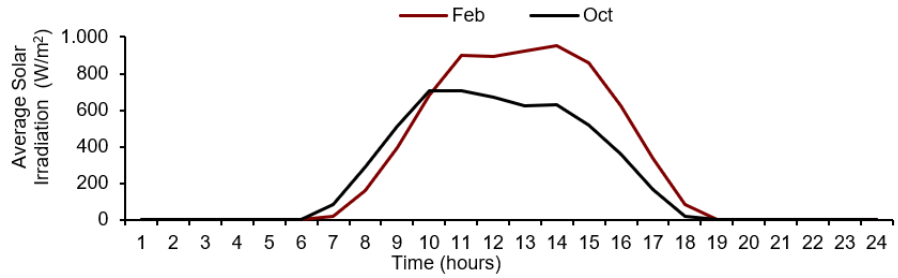

Fig. 1 - Average hourly solar irradiation per month (*IDEAM, 2020*)

RICE HUSK CHARACTERISTICS

Rice husk is a biomass or plant tissue consisting of cellulose, silica, among other elements that allows its use as fuel. This biomass has a great potential for energy in Colombia, due to its large production in the country and in its Caribbean coast (*Jaider et al., 2009*). Table 1 shows the most important characteristics for the technical and environmental analysis of this research.

Table 1

Rice husk characteristics (*Sánchez Lario, 2017; UPME, 2016b*)

% Humidity	$LHV_{biomass}$ (kJ/kg)	LHV_{biogas} (kJ/Nm^3)	Volume biogas per kg of biomass (Nm^3/kg biomass)	Emission factor $C_{em\ biogass}$ (Kg CO_2/kJ)	Emission factor $C_{em SO_2}$ (Kg SO_2/kJ)
10	14090	5330	0.92	0.103	0.000000153

ABSORPTION CHILLER CONFIGURATION

Figure 2 shows the simplified configuration scheme of the single-effect absorption refrigeration system based on the Thermal LTC-10 series, which has a nominal cooling capacity of 352 kW and uses the water/LiBr mixture as the working fluid (*Absorsistem, 2014*). Where this water/LiBr solution is driven by the pump to the desorber. The thermal energy is supplied to the desorber from an external circuit which includes solar thermal collectors and a gasifier.

In stream 7, superheated water vapor exits the desorber and, in stream 4, a lean water/LiBr solution leaves the desorber. Then, in the condenser, the water vapor is cooled by the water corresponding to stream 16. After the water exits the condenser, the fluid passes through the valve and its temperature decreases due to the expansion that occurs. Finally, the water enters the evaporator to cool stream 18, which is water that will extract heat from the conditioned space.

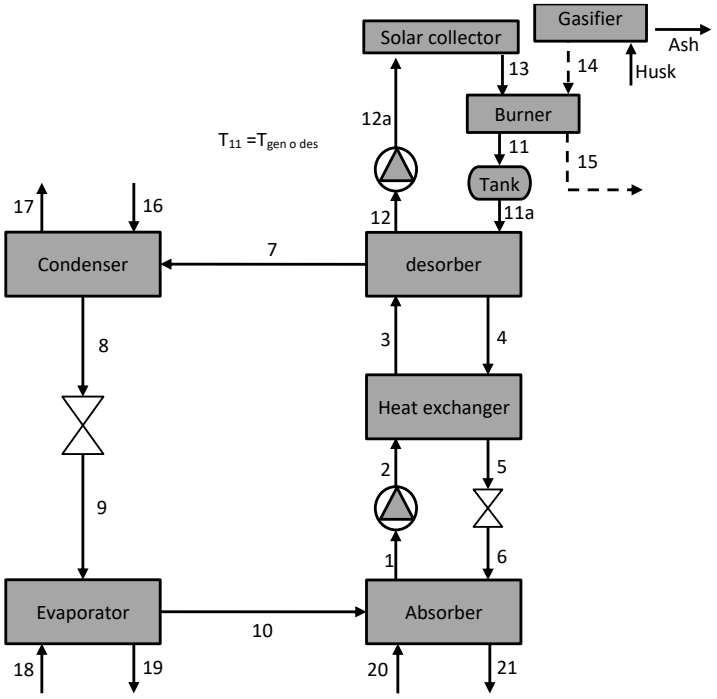

Fig. 2 - Absorption refrigeration system, solar collectors, and gasifier

The scenarios of the absorption refrigeration system are:

1. Solar-powered: The cooling system is solar-powered using Evacuated Tube Thermal Collectors.
2. Activated with rice husk biogas: The absorption refrigeration system is activated only with the biogas produced by rice husk gasification.
3. Activated with solar energy and biogas from rice husk: The absorption cooling system is activated with solar energy using the ETC collectors and the burning of biogas from the gasification of rice husk.
4. Conventional electricity-activated cooling system: This scenario is only evaluated to determine the emissions of greenhouse gases (CO_2 eq) and the equivalent amount of sulfur dioxide due to electrical energy consumed by a conventional system. This to compare the environmental effects of the previous scenarios with the conventional system.

THERMODYNAMIC MODEL

The thermodynamic system was analyzed with EES software. The properties of the working fluid were taken from the previous work of Pátek & Klomfar (*Pátek & Klomfar, 2006*) and provided to the EES software. The considerations of the thermodynamic evaluation are:

1. The temperature of the water at the evaporator inlet (stream 18) is 12 ºC.
2. The temperature of the water at the condenser inlet (stream 16) is 29.4 ºC (*Absorsistem, 2014*).
3. The temperature of the water at the absorber inlet (stream 20) is 29.4 ºC (*Absorsistem, 2014*).
4. The flow of water entering the condenser (50 m^3/h), absorber (50 m^3/h), desorber (74.9 m^3/h) and evaporator (55 m^3/h) is taken from the manufacturer's catalog, and the flows of water to the condenser and coming from the absorber have a parallel configuration (*Absorsistem, 2014*). The mass flow rate is calculated by multiplying the density of the water by the flow rate at the corresponding pressure and temperature.
5. For scenario 2 and 3, the water temperature at the outlet of the gas burner is 90ºC.
6. The water pressure entering the condenser and absorber is 105 kPa.
7. The pressure of the water entering the desorber is 500 kPa.
8. The pressure of the water entering the solar thermal collectors is 454.9 kPa.

9. The mass flow rate $\dot{m}_1$ is 1.681 kg/s.

10. The low system pressure is the saturation pressure of the water at T_{10} and the high system pressure is the saturation pressure of the water at T_8.

11. The refrigerant flow in the desorber (stream 7) is vapor and losses into the pipelines are negligible (*Rodríguez-Toscano et al., 2022b*).

12. The LHV_{biogas} is 14090 kJ/kg, the LHV_{biogas} is 5330 kJ/Nm^3 and the volume biogas is 0.92 Nm^3/kg biomass.

13. Thermal collector area (ETC) is 840.4 m^2.

14. The efficiency of the gasifier is 0.7 (*Sánchez Lario, 2017*).

15. The efficiency of the gas heater (η_{GN}) is 0.85 (*Gomri, 2013*).

16. The length of the heat reservoir is considered equal to its diameter (*Bellos et al., 2017*).

17. The efficiency of the solution pump is 0.6.

18. The effectiveness of the Evaporator is 0.815 (*Rodríguez-Toscano et al., 2022a*), the effectiveness of the condenser is 0.676 (*Rodríguez-Toscano et al., 2022a*), the effectiveness of the absorber is 0.5 *(Rodríguez-Toscano et al., 2022a*), the effectiveness of the desorber is 0.302 (*Rodríguez-Toscano et al., 2022a*) and the effectiveness of the exchanger is 0.64 (*Rodríguez-Toscano et al., 2022a*).

19. The thermal reservoir is adiabatic (*Rodríguez-Toscano et al., 2022a*).

20. Thermodynamic evaluation is performed between 7:00 and 20:00 hours.

21. The thermodynamic model has been previously validated by one of the present authors (*Rodríguez-Toscano et al., 2022a*). Table 2 provides the mass and energy balance equations of the absorption chiller.

Table 1

Mass and energy balances of the absorption chiller

Components	Mass Balance	Eq.	Ref.	Energy balance and	Eq.	Ref.
Solar thermal collector	$\dot{m}_{12a} = \dot{m}_{13}$	1	-	$\dot{Q}_s = A_c I_s$ A_c is the area of thermal solar collectors in m^2. I_s is the solar radiation in W/ m^2	17	(*Kalogirou, 2004*)
				$\eta_c = \frac{\dot{Q}_u}{\dot{Q}_s} = \frac{\dot{m}_{11} c_p (T_{12} - T_{13})}{A_c I_s}$	18	-
				$\eta_c = n_o - \frac{a_1 \Delta T_{avg}}{I_s} - \frac{a_2 (\Delta T_{avg})^2}{I_s}$ n_o=0.82 a_1=2.198 a_2=0	19	(*Asadi et al., 2018; Bellos et al., 2017; Rodríguez-Toscano et al., 2022b*)
Pump	$\dot{m}_1 = \dot{m}_2$	2	-	$\dot{W}_p = \eta_p \cdot \dot{W}_{p\,el}$ where η_p is the pump efficiency	20	-
				$\dot{W}_p = \dot{m}_1 \cdot \upsilon_1 \cdot (P_2 - P_1)$	21	-
Heat Exchanger	$\dot{m}_2 = \dot{m}_3$	3	-	$\dot{Q}_{shx} = \dot{m}_2 \cdot (h_3 - h_2)$	22	-
	$\dot{m}_4 = \dot{m}_5$	4	-	$\dot{Q}_{shx} = \dot{m}_4 \cdot (h_4 - h_5)$	23	-
				$\varepsilon = \frac{T_4 - T_5}{T_4 - T_2}$	24	-
Desorber	$\dot{m}_3 = \dot{m}_7 + \dot{m}_4$	5	-	$\dot{Q}_d = \dot{Q}_u + \dot{Q}_{GN}$	25	(*Gomri, 2013*)
	$\dot{m}_3 X_3 = \dot{m}_7 + \dot{m}_4 X_4$ where X is the concentration of LiBr in the solution.	6	-	$\dot{Q}_{GN} = \frac{\dot{m}_{GN} \cdot LHV_{biogas} \cdot \eta_{GN}}{\rho_{biogas\ per\ kg\ of\ biomass}}$	26	-
				$\dot{Q}_{GN} = \dot{m}_{11} \cdot C_p \cdot (T_{11a} - T_{13})$	27	-
				$\dot{Q}_d = \dot{m}_7 \cdot h_7 - \dot{m}_3 \cdot h_3 + \dot{m}_4 \cdot h_4$	28	-
				$\dot{Q}_d = \dot{m}_{11} \cdot C_p \cdot (T_{11a} - T_{12})$	29	-
				$\varepsilon = \frac{T_4 - T_3}{T_{11a} - T_3}$	30	-

Components	Mass Balance	Eq.	Ref.	Energy balance and	Eq.	Ref.
Absorber	$\dot{m}_{10} = \dot{m}_1 - \dot{m}_6$ $\dot{m}_6 X_6 + \dot{m}_{10} = \dot{m}_{10} X_{10}$. where X is the concentration of LiBr in the solution.	7	-	$\dot{Q}_a = \dot{m}_{10} \cdot h_{10} + \dot{m}_6 \cdot h_6 - \dot{m}_1 \cdot h_1$	31	-
				$\dot{Q}_a = \dot{m}_{20} \cdot C_p \cdot (T_{21}\text{-}T_{20})$	32	-
				$\varepsilon = \frac{T_6 - T_1}{T_6 - T_{20}}$	33	-
Condenser	$\dot{m}_7 = \dot{m}_8$	8	-	$\dot{Q}_{cond} = \dot{m}_7 \cdot h_7 - \dot{m}_8 \cdot h_8$	34	-
				$\dot{Q}_{cond} = \dot{m}_{16} \cdot C_p \cdot (T_{17} - T_{16})$	35	-
				$\varepsilon = \frac{T_7 - T_8}{T_7 - T_{16}}$	36	-
Evaporator	$\dot{m}_9 = \dot{m}_{10}$	9	-	$\dot{Q}_e = \dot{m}_{10} \cdot h_{10} - \dot{m}_9 \cdot h_9$	37	-
				$\dot{Q}_e = \dot{m}_{18} \cdot C_p \cdot (T_{18} - T_{19})$	38	-
				$\varepsilon = \frac{T_{18} - T_{19}}{T_{18} - T_{19}}$	39	-
Valve 1	$\dot{m}_8 = \dot{m}_9$	10	-	$h_8 = h_9$	40	-
Valve 2	$\dot{m}_5 = \dot{m}_6$	11	-	$h_5 = h_6$	41	-
The heat reservoir tank	$V_{tank} = \frac{A_c}{30}$	12	(Asadi et al., 2018)	-	42	(*Bellos & Tzivanidis, 2017*)
Gasifier	$\dot{m}_{GN} = \dot{m}_{14}$	13	-	$\eta_{gasifier} = \frac{\dot{Q}_{gasifier}}{\dot{Q}_{husk}}$ $\eta_{gasifier} = \frac{}{\rho_{biogas\ per\ kg\ of\ biomass}\ LHV_{biogas}}$	43	(*Sánchez Lario, 2017*)
	$\dot{m}_{ash} = 0.005 \frac{kg\ ash}{kg\ biom} \cdot \dot{m}_{husk}$	14	(Sánchez Lario, 2017)	$\dot{Q}_{gasifier} = \frac{\dot{m}_{GN}\ LHV_{biogas}}{\rho_{biogas\ per\ kg\ of\ biomass}}$	44	(*Sánchez Lario, 2017*)
				$\dot{Q}_{husk} = \dot{m}_{husk}\ LHV_{husk}$	45	(*Sánchez Lario, 2017*)
Absorption cooling system	-	15	-	$COP = \frac{\dot{Q}_{ev}}{\dot{Q}_d + \dot{W}_p}$ The COP is the coefficient of performance of the absorption	46	(*Rodríguez-Toscano et al., 2022a*)
Total system	-	16	-	$COP_{system} = \frac{\dot{Q}_{ev}}{\dot{Q}_s + \dot{Q}_{husk} + \dot{W}_{p\ el}}$	47	-

Eq. 48 defines the CO_2eq emissions, and the environmental effects associated to the use of biogas (scenario 3) (*Comisión del Cambio Climático, 2011; Rodríguez-Toscano et al., 2022b*).

$$CO_2\ eq = (\dot{m}_{GN} \cdot C_{em\ biogass} + \dot{W}_e \cdot C_{em\ el}) \cdot time_{use} \quad (48)$$

where: $C_{em\ el}$ is the emission factor of kg of CO_2 associated to the electricity consumption (kW-h) and it is equal to 0.181 kg CO_2 / kWh. The above equation also applies to scenario 2.

In this sense, Eq. 49 calculates the CO_2eq emissions associated to the energy consumption (scenario 4) (*Comisión del Cambio Climático, 2011; Rodríguez-Toscano et al., 2022b*).

$$CO_2eq = (\dot{Q}_e / (COP_{comp}) \cdot time_{use} \cdot C_{em\ el} \quad (49)$$

COP_{comp} is assumed as 3 *(Bellos & Tzivanidis, 2017; Rodríguez-Toscano et al., 2022a*).

Then, Eq. 50 determines the CO_2eq associated with the energy consumption (scenario 1) (*Comisión del Cambio Climático, 2011; Rodríguez-Toscano et al., 2022b*).

$$CO_2\ eq = \dot{W}_e \cdot time_{use} \cdot C_{em\ el} \quad (50)$$

Last but not least, Eq. 51 calculates the SO_2eq associated to the biogas burning (scenario 2 and 3).

$$SO_2\ eq = \dot{Q}_{gasifier} \cdot time_{use} \cdot C_{em SO_2} \quad (51)$$

RESULTS

Figure 3a shows the heat rate used to activate the desorber versus the solar energy potential and the biomass energy of the rice husk. In this figure, scenario 1 has the best ratio between 8:00 and 16:00 hours, since this is the period with the highest solar irradiation and the highest efficiency of the ETC's (0.66). Furthermore, the COP (see Figure 3b.) presents the highest value presented and hence the highest $\dot{Q}e$ of all scenarios. However, this system can only operate until 17:00 hours. Concerning scenario 2, the ratio (see Figure where X is the concentration of LiBr in the solution. 3a) and COP (see Figure 3b) remain constant throughout the operating hours. In general, if the area under the curve is considered, it is in this scenario where the energy potential during the entire operating time is used to the greatest extent. Scenario 3 exceeds the ratio of scenario 2 only between 9:00 and 12:00 hours and throughout the timetable it presents practically the same COP. With this behavior, the system in scenario 3 could improve the heat transfer in the absorber. The above would imply further increasing the biomass mass flow between 07:00 and 08:00 and between 16:00 and 20:00 hours.

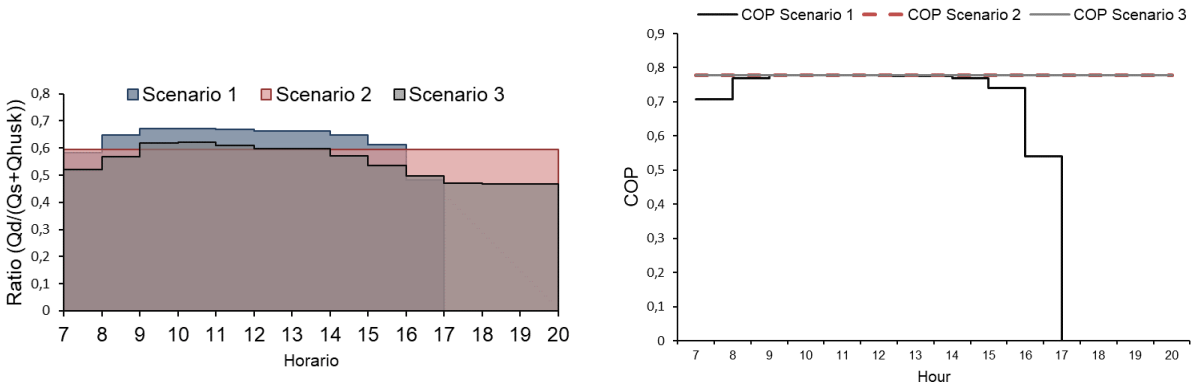

Fig. 3 - Heat rate and COP analysis of the thermodynamic system

a) Desorber rate in relation to the potential of energy sources.
b) COP of the absorption refrigeration system for the different scenarios

After maintaining the highest value, the COP_{system} develops a downward concavity curve as the system increases the amount of $\dot{Q}e$ relative to the amount of $\dot{Q}s$ at peak hours. It should be noted that the COP_{system} is changing continuously due to the indicator variation without a backup (note that $\dot{Q}_e$ has a lower value compared to other scenarios due to the quantity of solar collectors and solar energy at time). For scenario 3, the COP_{system} maintains the highest value during off-peak hours. Between 7:00 and 8:00 hours the COP_{system} is 0.4 and between 15:00 and 16:00 hours the COP_{system} is 1.36. Between 16:00 hours and 17:00 hours, the COP_{system} takes a value of 0.38. After 17:00 hours, this value is equal to 0.37. This behavior is expected because the decrease in the COP_{system} indicator is generated by the participation of rice husk biogas in the constant temperature combustion with the least amount of solar energy available at the same time. The above is supported by comparing the behavior of the scenario 3 with Figure 1. The COP_{system} curve is concaved upward as the amount of solar energy is higher at peak hours for $\dot{Q}_d$. The constant behavior of $\dot{Q}_e$ is because the gas burner works at a constant temperature (this is because the burner operates to maintain a constant temperature in the water at T11).

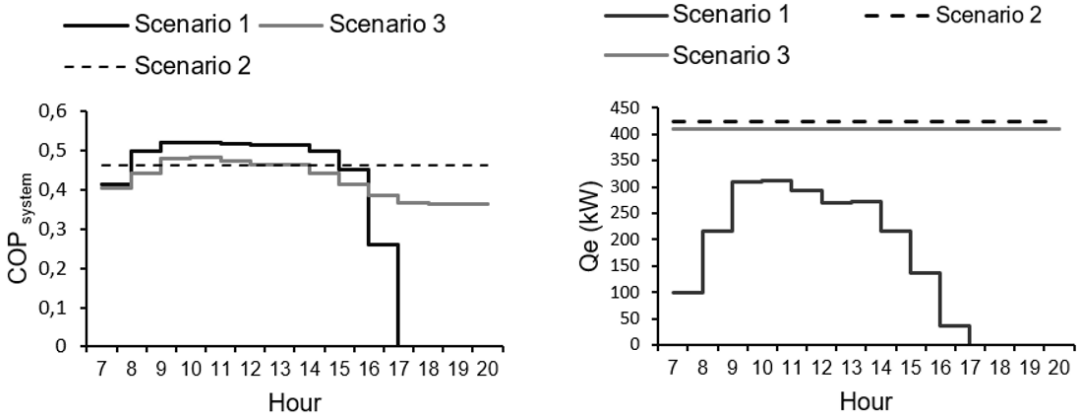

Fig. 4 - Analysis of the COP_{system} and $\dot{Q}_e$ for each scenario

a) COP_{system} of the total system for scenarios 1,2 and 3. b) $\dot{Q}_e$ of the absorption refrigeration system

Figure 5 shows the amount of biomass required to activate the rice husk absorption refrigeration system in the scenarios 2 and 3. In general, to activate the system at nominal capacity, 0.064 kg/s is required. For the scenario 2, the mass flow remains constant value of 0.064 kg/s. In the case of scenario 3, the amount of biomass mass flow decreases due to the significant solar energy input during the hours of sunshine (between 7:00 and 17:00 hours). This allows flexibility in the nominal range of the system using rice husk of up to 71.7%.

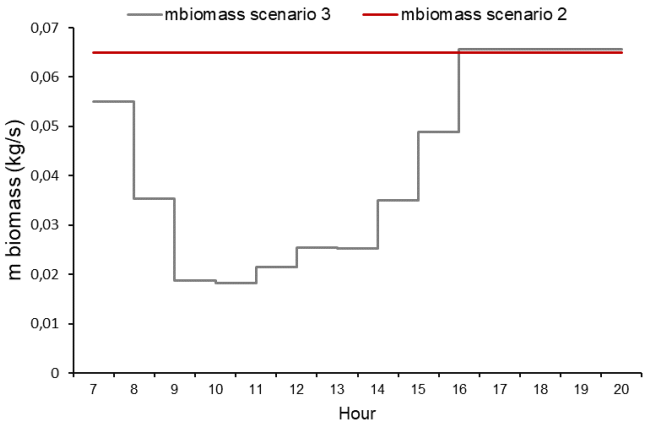

Fig. 5 - Mass flow of rice husk in scenario 2 and 3

GREENHOUSE GASES AND SULFUR DIOXIDE SO_2

Figure 6a shows the GHGs for each scenario. The scenario 4 was evaluated with respect to the other scenarios to propose an objective comparison of the results and determine the decrease of GHGs. The absorption refrigeration system that achieved the greatest reduction in relation to the conventional system was the first described in scenario 1 (99.98%), followed by the scenario 3 (99.6%) and the scenario 2 (99.53%). This behavior is explained using another energy source (rice husk) which causes GHGs in a low amount. Figure 6b shows the amount of sulfur dioxide produced for scenarios 1, 2 and 3. The results show that the System evaluated in scenario 1 does not generate sulfur dioxide. Although scenarios 2 and 3 generate the highest values of sulfur dioxide, these amounts are low and do not tend to significantly pollute the surrounding environment. In these cases, filters should be used according to humidity and particulate matter to avoid the formation of aerosols over time.

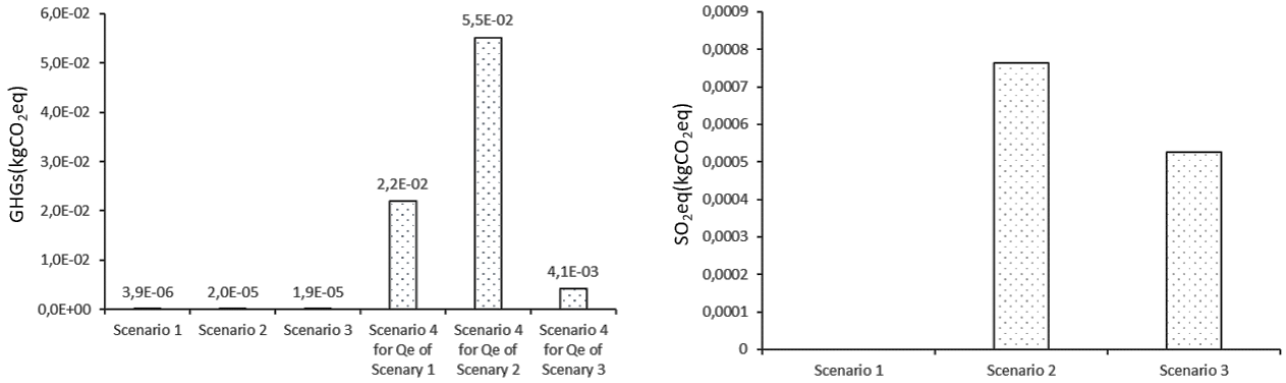

Fig. 6 - Analysis of greenhouse gases and sulfur dioxide emissions

a) GHGs or CO_2 eq for the various scenarios. b) SO_2 eq for the several scenarios.

CONCLUSIONS

The absorption cooling systems using solar energy (with ETC) and biomass (rice husk) as energy sources are technically feasible. However, only scenarios 2 and 3 can operate throughout the proposed schedule. The system evaluated in scenario 1 operates between 7:00 and 17:00 hours with the partial or nominal evaporator cooling load for the typical day of the most critical month. The COP and COP_{system} are highest at peak hours. In addition, this is the scenario that provides the greatest reduction in GHGs.

The system evaluated in scenario 1 presented the greatest reduction of GHGs and the maximum COP and COP_{system} in relation to $\dot{Q}_e$. If the technical and environmental benefits such as flexibility or availability of the energy source, the COP, the $COP_{system,}$ the amount of GHGs and the amount of sulfur dioxide are compared and the behavior of a compression (conventional) cooling system is analyzed, the most favorable option is the absorption refrigeration system that uses both energy sources (scenario 3). If only the technical aspects and GHGs are taken into consideration, the best option is the technology that uses solar energy (scenario 1). However, this analysis does not consider the investment and operating costs of the entire system. Therefore, further studies may consider an assessment of these scenarios from an economic perspective.

Concerning the rate of energy used by the desorber and the potential energy for its activation ($\dot{Q}s+\dot{Q}husk$), this variable maintained a constant value in scenario 2. The system evaluated in scenario 3 only surpassed the indicator (ratio) corresponding to the system of scenario 2, between 9:00 and 12:00 hours. As for the scenario 1, in peak hours it outperformed all of them. Therefore, it is identified that a control and resource management strategy can be generated to improve the use of the energy needed to activate the cooling system by reducing the amount of rice husk while using more solar energy during peak hours. Finally, for the absorption refrigeration system of scenario 3, it is recommended to study in future research the amount of ETC to find an optimal operating condition that favors economic feasibility.

ACKNOWLEDGEMENT

The authors are very thankful to the Universidad de la Costa and MINCIENCIAS. This study is part of a research project funded by the named institutions through the INDEX project CONV-13-2018 and CONV-15-2020.

REFERENCES

[1] Adel, J., AlFaris, F., Montoya, F., & Manzano-Agugliaroa, F. (2016). Energy benchmarking for shopping centers in Gulf Coast region. *Energy Policy*, 247–255.

[2] Alhamid, M. I., Coronas, A., Lubis, A., Ayou, D. S., Nasruddin, Saito, K., & Yabase, H. (2020). Operation strategy of a solar-gas fired single/double effect absorption chiller for space cooling in Indonesia. *Applied Thermal Engineering*, *178*. https://doi.org/10.1016/j.applthermaleng.2020.115524

[3] Allouhi, A., Kousksou, T., Jamil, A., Bruel, P., Mourad, Y., & Zeraouli, Y. (2015). Solar driven cooling systems: An updated review. *Renewable and Sustainable Energy Reviews*, *44*, 159–181. https://doi.org/10.1016/j.rser.2014.12.014

[4] Amaris, C. C. (2013). *Intensification of NH 3 Bubble Absorption Process using Advanced Surfaces and Carbon Nanotubes for NH 3 /LiNO 3 Absorption Chillers*.

[5] Asadi, J., Amani, P., Amani, M., Kasaeian, A., & Bahiraei, M. (2018). Thermo-economic analysis and multi-objective optimization of absorption cooling system driven by various solar collectors. *Energy Conversion and Management*, *173*(July), 715–727. https://doi.org/10.1016/j.enconman.2018.08.013

[6] Aune, M., Godbolt, Å. L., Sørensen, K. H., Ryghaug, M., Karlstrøm, H., & Næss, R. (2016). Concerned consumption. Global warming changing household domestication of energy. *Energy Policy*, *98*, 290–297. https://doi.org/10.1016/j.enpol.2016.09.001

[7] Ayou, D. S., Bruno, J. C., Saravanan, R., & Coronas, A. (2013). An overview of combined absorption power and cooling cycles. In *Renewable and Sustainable Energy Reviews* (Vol. 21, pp. 728–748). Pergamon. https://doi.org/10.1016/j.rser.2012.12.068

[8] Bellos, E., & Tzivanidis, C. (2017). Energetic and financial analysis of solar cooling systems with single effect absorption chiller in various climates. *Applied Thermal Engineering*, *126*, 809–821. https://doi.org/10.1016/j.applthermaleng.2017.08.005

[9] Bellos, E., Tzivanidis, C., Symeou, C., & Antonopoulos, K. A. (2017). Energetic, exergetic and financial evaluation of a solar driven absorption chiller – A dynamic approach. *Energy Conversion and Management*, *137*, 34–48. https://doi.org/10.1016/j.enconman.2017.01.041

[10] Castro, A. O. (2010). Análisis del potencial energético solar en la Región Caribe para el diseño de un sistema fotovoltaico. *INGE CUC*, *6*(1), 95–102.

[11] Ghafoor, A., & Munir, A. (2015). Worldwide overview of solar thermal cooling technologies. *Renewable and Sustainable Energy Reviews*, *43*, 763–774. https://doi.org/10.1016/j.rser.2014.11.073

[12] Gomri, R. (2013). Simulation study on the performance of solar/natural gas absorption cooling chillers. *Energy Conversion and Management*, *65*, 675–681. https://doi.org/10.1016/j.enconman.2011.10.030

[13] Jaider, E.C., Aguilar, S., De, U., Facultad, S., & Ingenieria, D. E. (2009). *Alternativas de aprovechamiento de la cascarilla de arroz*.

[14] Juaidi, A., Al Faris, F., Montoya, F. G., & Manzano-Agugliaro, F. (2016). Energy benchmarking for shopping centers in Gulf Coast region. *Energy Policy*, *91*, 247–255. https://doi.org/10.1016/j.enpol.2016.01.012

[15] Kalogirou, S. A. (2004). Solar thermal collectors and applications. In *Progress in Energy and Combustion Science* (Vol. 30, Issue 3, pp. 231–295). Pergamon. https://doi.org/10.1016/j.pecs.2004.02.001

[16] Li, K., Xiong, P., Wu, Y., & Dong, Y. (2022). Forecasting greenhouse gas emissions with the new information priority generalized accumulative grey model. *Science of the Total Environment*, *807*, 150859. https://doi.org/10.1016/j.scitotenv.2021.150859

[17] Pátek, J., & Klomfar, J. (2006). A computationally effective formulation of the thermodynamic properties of LiBr-H2O solutions from 273 to 500 K over full composition range. *International Journal of Refrigeration*, *29*(4), 566–578. https://doi.org/10.1016/j.ijrefrig.2005.10.007

[18] Pérez-Lombard, L., Ortiz, J., & Pout, C. (2008). A review on buildings energy consumption information. *Energy and Buildings*, *40*(3), 394–398. https://doi.org/10.1016/J.ENBUILD.2007.03.007

[19] Rodríguez-Toscano, A., Amaris, C., Sagastume-Gutiérrez, A., & Bourouis, M. (2022a). Technical, environmental, and economic evaluation of a solar/gas driven absorption chiller for shopping malls in the Caribbean region of Colombia. *Case Studies in Thermal Engineering*, *30*, 101743. https://doi.org/10.1016/J.CSITE.2021.101743

[20] Rodríguez-Toscano, A., Amaris, C., Sagastume-Gutiérrez, A., & Bourouis, M. (2022b). Technical, environmental, and economic evaluation of a solar/gas driven absorption chiller for shopping malls in the Caribbean region of Colombia. *Case Studies in Thermal Engineering*, *30*, 101743. https://doi.org/10.1016/j.csite.2021.101743

[21] Sagastume Gutiérrez, A., Cabello Eras, J. J., Hens, L., & Vandecasteele, C. (2020). The energy potential of agriculture, agroindustrial, livestock, and slaughterhouse biomass wastes through direct combustion and anaerobic digestion. The case of Colombia. *Journal of Cleaner Production*, *269*, 122317. https://doi.org/10.1016/j.jclepro.2020.122317

[22] Saint Akadiri, S., Adewale Alola, A., Olasehinde-Williams, G., & Udom Etokakpan, M. (2020). The role of electricity consumption, globalization and economic growth in carbon dioxide emissions and its implications for environmental sustainability targets. *Science of the Total Environment*, *708*, 134653. https://doi.org/10.1016/j.scitotenv.2019.134653

[23] Sánchez Lario, A. (2017). *Diseño de una planta de gasificación con cogeneración para el aprovechamiento energético de la cascarilla de arroz en un proceso industrial*. E.T.S.I. Diseño Industrial (UPM).

[24] Toscano, A. D. R., Torres, D. A. A., Pérez, D. M., Castillo, A. P. P., Herazo, J. C. M., & Rivera, M. H. (2021). Estimation and Trends of the Absorption Refrigeration Global Market. *Smart Innovation, Systems and Technologies*, *205*, 633–643. https://doi.org/10.1007/978-981-33-4183-8_50

[25] Toscano, A. R., Piñeres Castillo, A. P., Mojica Herazo, J. C., López, R. L., & Restrepo, R. R. (2020). Management and Control of Variables for the Generation of Biogas from Pig Zungo. *Procedia Computer Science*, *177*, 261–266. https://doi.org/10.1016/J.PROCS.2020.10.036

[26] Zapata, A., Amaris, C., Sagastume, A., & Rodríguez, A. (2021). CFD modelling of the ammonia vapour absorption in a tubular bubble absorber with NH3/LiNO3. *Case Studies in Thermal Engineering*, *27*, 101311. https://doi.org/10.1016/J.CSITE.2021.101311

[27] ***Absorsistem. (2014). *Plantas enfriadoras de agua por ciclo de absorción, accionadas por agua caliente.* https://absorsistem.com/

[28] ***Comisión del Cambio Climático. (2011). *Guía práctica para el cálculo de emisiones de gases de efecto invernadero (GEI) GUÍA PRÁCTICA PARA EL CÁLCULO DE EMISIONES DE GASES DE EFECTO INVERNADERO (GEI)*.

[29] ***Empresas Públicas de Medellín (EPM). (2020). *Tarifario del mes | Gases del Caribe*. Tarifario Del Mes. https://gascaribe.com/tarifario-del-mes/

[30] ***Federación Nacional de Biocombustibles de Colombia. (2018, January 20). *Federación Nacional de Biocombustibles de Colombia*. Desperdicio Que Sí Sirve. https://www.fedebiocombustibles.com/nota-web-id-3016.htm

[31] ***Instituto de Hidrología, Meteorología y Estudios Ambientales (IDEAM). (2020). *Boletín Climatológico Mensual - CLIMATOLÓGICO MENSUAL - IDEAM*. http://www.ideam.gov.co/web/tiempo-y-clima/climatologico-mensual
[32] ***International Energy Agency (IEA). (2019). *Perspectivas energéticas mundiales 2019 - Análisis - IEA*. Perspectivas Energéticas Mundiales 2019. https://www.iea.org/reports/world-energy-outlook-2019#
[33] ***United States Department of Energy. (2016). *Absorption Chillers for CHP Systems*. 3–6.
[34] ***Unidad de Planeación Minero Energética (UPME). (2015). Integración de las energías renovables no convencionales en Colombia. In *Ministerio de Minas y Energía*. https://doi.org/10.1021/ja304618v
[35] ***Unidad de Planeación Minero Energética (UPME). (2016a). *Atlas del potencial energético de la Biomasa residual en Colombia*. Atlas Del Potencial Energético de La Biomasa Residual En Colombia. https://www1.upme.gov.co/siame/Paginas/atlas-del-potencial-energetico-de-la-biomasa.aspx
[36] ***Unidad de Planeación Minero Energética (UPME). (2016b). *FECOC*. Total de Emisiones CO2 Calculadas. http://www.upme.gov.co/calculadora_emisiones/aplicacion/calculadora.html
[37] ***Weather Underground. (2020). *Barranquilla, Colombia Weather Conditions | Weather Underground*. https://www.wunderground.com/weather/co/barranquilla